Evolving a Psycho-physical Distance Metric for Generative Design Exploration of Diverse Shapes

Shahroz Khan*,[1] Erkan Gunpinar[2] Masaki Moriguchi[3] Hiromasa Suzuki[1]
[1] The University of Tokyo, Tokyo, Japan
[2] Istanbul Technical University, Istanbul, Turkey
[3] Meiji University, Tokyo, Japan

Abstract

In this paper, a generative design approach is proposed that involves the users' psychological aspect in the design space exploration stage to create distinct design alternatives. Users' perceptual judgment about designs is extracted as a psycho-physical distance metric, which is then integrated into the design exploration step to generate design alternatives for the parametric computer-aided design (CAD) shapes. To do this, a CAD model is first parametrized by defining geometric parameters and determining ranges of these parameters. Initial design alternatives for the CAD model are generated using Euclidean distance-based *Sampling Teaching-Learning-Based Optimization* (S-TLBO), which is recently proposed and can sample *N* space-filling design alternatives in the design space. Similar designs are then clustered and a user study is conducted to capture the subjects' perceptual response for the dissimilarities between the cluster pairs. Additionally, a furthest-point-sorting technique is introduced to equalize the number of designs in the clusters, which are being compared by the subjects in the user study. Afterward, nonlinear regression analyses are carried out to construct a mathematical correlation between the subjects' perceptual response and geometric parameters in the form of psycho-physical distance metric. Finally, a psycho-physical distance metric obtained is utilized to explore distinct design alternatives for the CAD model. Another user study is designed to compare the diversification between the designs when the Euclidean and suggested psycho-physical distance metrics are utilized. According to the user study, designs generated with the latter metric are more distinct.

Keywords: Generative Design, Computer-Aided Design, Parametric Design, Space-filling, S-TLBO method

1. Introduction

The development of a successful product involves a series of design phases. Among these phases, the conceptual phase mostly is recognized as a foundational and fundamental component. The exploration and formulation of different design options within the product's design specifications are an important characteristic of this phase. At this phase, it is essential for the designers/engineers to explore and develop a wide variety of creative and ingenious designs/solutions to a product/problem. However, the creation of these alternatives using the traditional design tools is a time-consuming and difficult task, especially for novice designers, but with the recent advancements in the artificial intelligence, design optimization, and parametric techniques the traditional design tools are becoming sophisticated and intuitive.

The generative design systems use these techniques to provide a promising way to iterate through variant design alternatives based on the user-defined objective. However, despite the proven feasibility of the generative design systems in term of exploring better performance design options, the literature contains few attempts to utilize these systems to explore design alternatives for the parametric CAD models specifically on account of their form appearance. The generative design systems such as DesignN [1] Genoform [2] and Autodesk's Fractal [3] explore parametric space for shape variation, however, among these, [2] and [3] are based on the exhaustive and iterative search techniques to induce variation between designs, respectively. Therefore, due to their exhaustive and iterative search nature, these techniques can only explore a limited region of design space and thus cannot always guarantee the generation of diverse and appealing design options for the designers.

At the conceptual design phase, it is also crucial for a designer to create a product that not only satisfies design specifications but also meets the customers' psychological preference of the product's appearance to make the product successful within the market. The customers' psychological satisfaction with a product drives significantly from its form appearance. Therefore, an important element of the design exploration process should be the consideration of the psychological aspect of a product, including the visual perception of the potential user to the proposed design alternatives for the product. Therefore, the prime objective of this work is to develop a technique that can effectively explore a design space and recommend/sample aesthetically convincing and diverse design alternatives for a product at the conceptual phase of the design process. In which diversification between designs is achieved with a psycho-physical metric evolved from the users' perception of the design alternatives.

To achieve the above objective, in this work, a generative design approach is proposed which integrates a psycho-physical

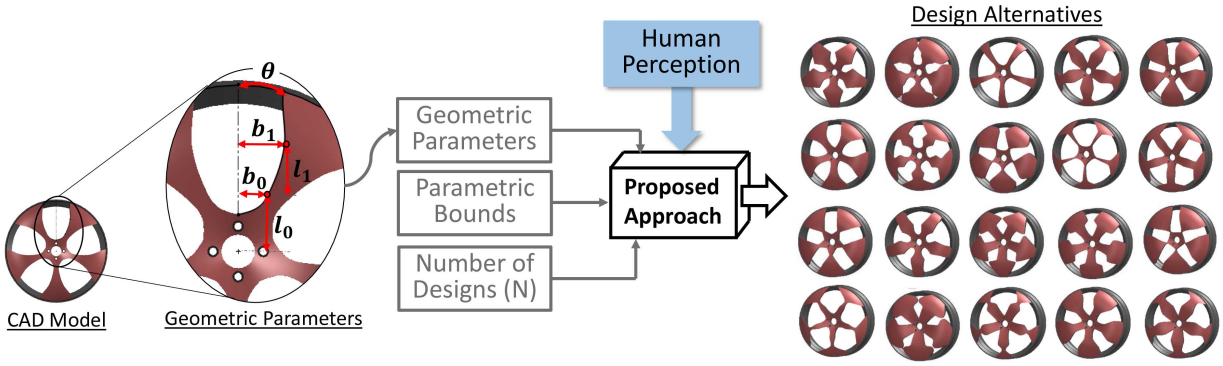

Figure 1: Overview of the proposed approach.

distance metric to induce human perception for the design diversification during the design space exploration. This approach is based on a newly introduced CAD model sampling technique called Sampling-TLBO (S-TLBO) [4], which uses a Teaching-Learning-Based Optimization (TLBO) technique [5] to find the N optimal space-filling design alternatives for a given model within the class of semi-Latin Hypercube (LH) designs. Figure 1 shows an overview of the proposed approach.

The proposed approach commences by representing a CAD shape with a set of appropriate geometric/design parameters (see Figure 1). A design space is formed by setting the upper and lower bounds to the geometric parameters. Each geometric parameter represents a dimension in the design space. The design alternatives for the CAD model are created in the design space while considering the space-filling and non-collapsing criterion via S-TLBO. To learn the psycho-physical distance metric for the parametric shape, user studies were conducted between subjects of varying backgrounds. First, N initial design alternatives of the CAD model are generated using S-TLBO, and similar designs are then clustered. Afterward, the user study is conducted in which subjects are asked to indicate their perceptual response about the relative degree of dissimilarity between each pair of clustered designs. To ease subjects during the study, the size of comparing cluster pairs are equalized using a new *furthest-point-sorting* technique. The statistical analysis such as nonlinear regression was performed to learn a psycho-physical relationship between geometric parameters and users' perceptual response about design dissimilarities. The mathematical model obtained was then regarded as a psycho-physical distance metric. The results were also validated through various statistical tests. Figure 2 shows the sequential flow of the implementation of the methods utilized to learn this metric. Finally, a comparative study was conducted to compare the sampling quality when the Euclidean and psycho-physical distance metrics are employed.

The main contribution of this work is the development of a novel perceptual model, psycho-physical distance metric, for design diversification and the integration of this model with the generative design to develop a design methodology, which can be used for the diverse design exploration of a given shape. Such design technique can help engineers and designers to create innovative and distinct designs during the conceptual phase of the design process, which can be later validated for functionality, structural integrity, and usability via computer simulations during the design validation phase. To the best of our knowledge, there is no generative design system/technique that integrates design diversification based on human perception into the *exploration of parametric design spaces.*

The remainder of this paper is organized as follows: Section 2 reviews relevant literature. Formulation of original S-TLBO algorithm is described in Section 3. Section 4 presents the extraction process of the psycho-physical distance metric. The numerical results for the test models of the proposed approach are given in Section 5. Concluding remarks and opportunities for future work are given in Section 6.

2. Related works

The research topic of this work is more related to generative design, the human perception in design and sampling for space-filling designs, thus discussed here.

2.1. Generative design

In the last decade, generative design systems gained tremendous attention in industry and academics and have served as an advanced design tool which automatized the design process from its conceptual phase to the final fabrication phase. Most of the researchers' efforts in this field to explore design alternatives for the parametric CAD models are related to the architectural application, and few other works are done on the development of system generative creation of a specific class of products.

Krish [2] proposed a generative design system called *Genoform* for design exploration of parametric shapes. In Genoform, designer iterate through the randomly generated designs from a design space. To create variant designs, the designer defines a threshold value, which is set on the Euclidean distance between the generated designs. A drawback of Genoform is that it is based on an exhaustive search and can explore a limited region of design space. This hinders designers from generating creative designs. Similar to Genoform, recently, a new system called *Fractal* [3] has been developed by Autodesk. Fractal is based on a simple iterative approach in which each parametric range is divided into a certain number of levels, and then Fractal enumerate through all design possibilities. For instance, for

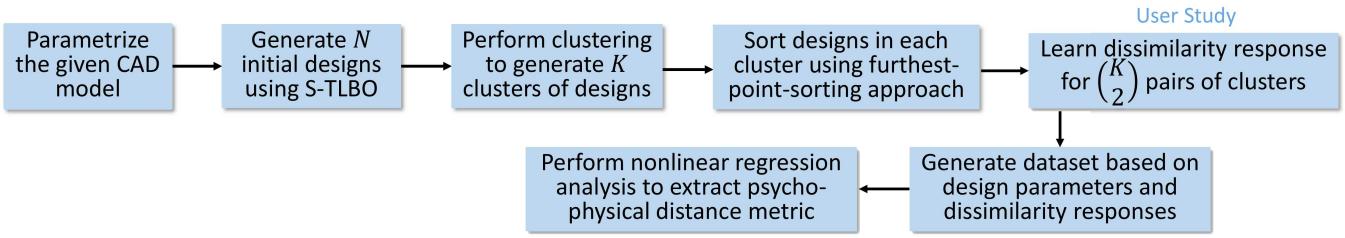

Figure 2: Flow of the proposed approach.

n geometric parameters each with I intervals, Fractal provides n^I design options. Recently, Gunpinar et al. [6] proposed a generative design system for the generation of Sedan Car Side Silhouettes. They also integrated their system with machine learning techniques to predict the drag coefficients of Car Silhouettes during design space exploration. Patel et al. [7] introduced a 3-dimensional (3D) sampling based generative design system called *3DJ* for synthesize new texture designs from 3D scenes. Another generative design system, *DreamSketch*, was proposed by Kazi et al. [8] to support the generative design in the conceptual phase. In DreamSketch, a user can create design alternatives in the sketched context. Therefore, to utilize this system, the user required to have digital sketching abilities. A design sampling technique was introduced by Gunpinar and Gunpinar [9] via particle tracing to create parametric space-filling designs. Hornby [10] and Barros et al. [11] utilized generative design techniques for furniture design. Khan et al. [12] suggested a spatial simulated annealing based generative design technique for creating customer-centered products. For an architectural application of generative design, Shea et al. [13] introduced a performance-driven generative design method to lightweight cantilever roof structures while integrating two generative structural design systems, *efiForm* and Bentley's *Generative Components*. Other architectural generative design systems are *ParaGen* and *Dexen* for exploring parametric structures and façade designs were introduced by Turrin et al. [14] and Patrick [15]. Moreover, different researchers have also developed generative design techniques to create building [16] and site [17] layouts and energy efficient building designs [18].

Many researchers have also developed shape grammars [19], L-systems [20] and component-based [21, 22] generative design systems for different applications. Shape grammars utilize a set of different geometric logics/rules to generate design alternatives for a given shape. Unlike shape grammars, in parametric-based design exploration processes, the important features of the design are selected/identified and parameterized with an appropriate set of geometric parameters. The variations of the input model are obtained by altering these parameters. On the other hand, in shape grammar design variations are generated by synthesizing different features into the initial design with the aid of geometric rules, which ensure the creation of feasible shapes [19]. Some common applications of shape grammars are architectural design [23], 2D automotive design [24], embroidery design [25], and wheel shapes with the integration of Finite Element Analysis (FEA) [26].

L-systems [27] are a variation of shape grammars, and utilize a set of production rules based on string rewriting mechanisms to formalize design alternatives. These systems have been utilized for different design problems such as generating realistic models of temperate-climate trees and shrubs [28] and complex building models [29]. In component-based synthesis techniques [21], a system is first trained using a large dataset of existing shapes. The system is then used to synthesize variant design alternatives.

Compare to shape grammar and component-based generative systems, parametric design exploration might restrain users from creating design alternative with a completely new feature because the initial design is parameterized based on that design features that are initially chosen by the user. In case of shape grammars, setting geometric rules at the conceptual design phase of a product can be time-consuming and cumbersome for a novice designer to explore feasible shapes if they are not available at hand. Ambiguous set of human-defined rules might also limit the designer to explore the design space for obtaining a satisfactory shape [30]. Furthermore, despite its different applications, shape grammar's usage is limited to industry. This is because of its computational complexity and requirement for forming a specific set of geometric rules for each application, which requires special expertise [2]. Moreover, the component-based systems [21] can only be used for creating alternatives of existing shape, which limits their implementation at the conceptual stage, because usually there may be no existing or a few CAD models at this stage [9]. Our technique can generate distinct designs based on the design features (initially chosen by the user) in the CAD model.

2.2. Human perception in design

Recently, the fusion of human perception into the design processes has gained notable attention from different research communities. Among many human perception criteria, design aesthetics is the well studied one. Many researchers have worked on design techniques to create aesthetically or stylistically optimal designs. For instance, Dev et al. [31] proposed a perceptual-based technique to compute a metric that gives an aesthetic ranking for a 3D shape. Their metric can be used to arrange the collection of design variations for shapes based on the aesthetics and provides user ability to identify and select the most aesthetic designs. A perception based style compatibility metric for furniture models was developed by Liu et al. [32] to generate compatible arrangements of furniture for 3D scenes. A similar metric was also developed by Lim et al. [33]

to measure the style similarity for a collection of designs. Secord et al. [34] proposed a perceptual model to find the goodness of a viewpoint for a 3D shape and Zhang et al. [35] also introduced a perceptual model for finding preferable 3D printing direction, which reduces the visual artifacts caused by the overhang supports. Recently, Hoshyari et al. [36] utilized human perception of shapes to create vector images of shapes, which maintains consistencies with the viewer's expectations. Tseng et al. [37] utilized artificial neural networks to quantitatively map the consumer judgments about the stylistic form of two-dimensional car designs and explored design space using multi-objective genetic algorithm while taking user's stylistic judgment and fuel consumption into account. In another study, Tseng et al. [38] studied the relationship of user quantified attributes for car design (such as sporty, rugged, aerodynamic and fuel efficient) to investigate how designers can generate designs that better represent consumer's desired goal.

A substantial amount of work has been done by different researchers to capture and involve customer's psychological perception in the product design process employing semantic attributes or Kansei-tags. In these techniques, a set of suitable attributes are first selected for a product. A mathematical model is then constructed to establish a correlation between the relative attribute and the product's form features. Chen and Chang [39] developed Kansei-tags for knife model. They conducted a user study to match the Kansei-tags with manually created different knife shape. They then performed a linear regression analysis to construct a linear relationship between each attribute and geometric parameters. Other researchers have done similar studies for cellular phone [40] and yacht [41] designs. Mata et al. [42] investigated the relationship between the user's perceptions and design aesthetics. The experiments were conducted using 11 different classes of vase designs and the results of the user study were analyzed using various statistical analyses. The identified relationships in [42] can help designers to determine important parameters in vase design and how these parameters can be altered to achieve concrete user perceptions. However, in [42] user perception about design diversification was not studied. User studies were conducted on the existing 2D vase and no parametric design exploration process was carried out.

Some researchers have also involved human perception into shape-synthesis techniques. Chaudhuri et al. [22] developed an attribute-based shape synthesis system called *Attriblt*. Models were first segmented into meaningful components. User studies were then conducted to learn the degree of a relative semantic attribute for each component. A machine learning model was trained to sort the degree of attributes, which was then used to synthesize new models by merging the components. As mentioned in Section 2.2, the shape-synthesis techniques can only be utilized when there is a dataset available consisting of different variations of the input shape.

Integration of customers' judgment in the optimization process along with the engineering performance objective was studied by Kelly et al. [43] and Villa and Labayrade [44]. Barnum and Mattson [45] presented an interactive and computationally assisted technique for capturing and incorporating designer preferences at the conceptual phase of the design process. Barnum and Mattson tested their method for different vehicle designs. Orsbon et al. [46] demonstrated the estimation of customer preferences as utility functions to obtain higher utility product forms and validated their technique for two-dimensional vehicle designs. Different researchers also proposed different interactive design techniques to involve designer preferences in the design process [47, 48].

Though there has been a considerable amount of effort in capturing and integrating human perception in various design applications, however, to the best of our knowledge, there has been no significant efforts in academia and industry to computationally integrate human perception about 3D design diversification into the *parametric design space exploration*.

2.3. Space-filling designs

Fuerle and Sienz [49] proposed a genetic algorithm based method to produce space-filling DoE in constrained spaces. This method has some drawbacks such that it cannot be implemented for high-dimensional problems more than $3D$. Furthermore, it does not produce good results for a design space where infeasible designs are spread irregularly. Cioppa and Lucas [50] introduced an algorithm for constructing orthogonal space-filling DoE in the class of Latin Hypercube design. However, their algorithm is computationally expensive because its long run times and is unsuitable for high-dimensional problems. Trosset [51] and Stinstra et al. [52] used maximin criterion for the construction of space-filling designs in the constrained 10-dimensional design space. The technique proposed by Stinstra et al. does not guarantee the sampled designs to be non-collapsing. Draguljić et al. [53] proposed a CoNcaD algorithm for constructing non-collapsing and space-filling designs for confined nonrectangular design spaces. However, S-TLBO can sample better space-filling designs compared to the methods mentioned above, which is proven in [4].

3. Sampling teaching-learning-based optimization (S-TLBO)

S-TLBO was originally proposed by Khan and Gunpinar [4] for the automatic search and generation of design variations for a CAD model in its predetermined design space. This technique is based on the Teaching-Learning-Based Optimization technique [5] and can generate N optimal designs in the constrained and unconstrained spaces. In S-TLBO, the sampling process starts by parameterizing the given CAD model with n geometric parameters $X = [x_1, x_2, x_3, \ldots, x_n]$. To create N distinct designs, S-TLBO randomly generates a population consisting of N sub-populations and improves learners/designs in these sub-populations using teaching and learning phases of typical TLBO. The best solution of each sub-population is regarded as a teacher. To obtain distinct designs, S-TLBO favors designs having space-filling and non-collapsing properties. Furthermore, the designs, which do not satisfy the predefined geometric constraints, are penalized using a weighted constraint handling mechanism. Space-filling designs are achieved by minimizing a Euclidean-distance based Audze and Eglais' potential energy [54] given in Equation 1. S-TLBO terminates

when there is no or negligible change in the cost function. After termination, teachers (T) of sub-populations are regarded as the sampled designs.

$$U(T) = \sum_{p=1}^{N-1} \sum_{q=p+1}^{N} \frac{1}{\sum_{j=1}^{n} (\overline{x}_{p,j} - \overline{x}_{q,j})^2} \quad (1)$$

In Equation 1, $U(T)$ is the potential energy of teachers T, $\overline{x}_{p,j}$ and $\overline{x}_{q,j}$ are the scaled values for j^{th} geometric parameter of design p and q, which are computed by scaling parameter values between 0 (i.e., lower bound for the parameter) and 1 (i.e., upper bound for the parameter). n and N are number of total geometric parameters and designs, respectively. Algorithm 1 summarizes the procedure of S-TLBO.

Algorithm 1 The pseudo-code of S-TLBO algorithm

1: Initialize the number of parameters (n), parameter ranges, number of designs to be created (N), sub-population size (s) and parameter α, which controls the degree of non-collapsingness between designs.
2: Randomly create an initial population (P) consisting of N sub-populations (p) of size s.
$P = \begin{bmatrix}(p_1)_{s\times n} & (p_2)_{s\times n} & (p_3)_{s\times n} & \dots (p_N)_{s\times n}\end{bmatrix}^T$ with $(p_L)_{s\times n} = \begin{bmatrix}X_1\\X_2\\\vdots\\X_s\end{bmatrix} = \begin{bmatrix}x_{1,1} & x_{1,2} & \dots & x_{1,n}\\x_{2,1} & x_{2,2} & \dots & x_{2,n}\\\vdots & \vdots & \vdots & \vdots\\x_{s,1} & x_{s,2} & \dots & x_{s,n}\end{bmatrix}$ where $1 \le L \le N$
3: Select N initial teachers/best-designs ($T = [T_1, T_2, \dots, T_N]$) one from each sub-population.
4: **while** termination criterion is not satisfied **do**
5: **for** $L = 1$ to N **do**
6: **for** $k = 1$ to s **do**
7: Update design X_k of $(p_L)_{s\times n}$ using Teacher and Learner phase based on T_L and obtain updated design X'_k.
8: Calculate cost value $U(T')$ and $U(T)$ for $T' = [X'_k, T_2, \dots, T_N]$ and $T = [X_k, T_2, \dots, T_N]$.
9: **if** $U(T') < U(T)$ **then**
10: Accept the design X'_k
11: **else**
12: Accept the design X_k
13: **end if**
14: **end for**
15: Update $(p_L)_{s\times n}$, which is $(p'_L)_{s\times n}$.
16: Find the new teacher T'_L and replace in T with T_L
17: **end for**
18: **end while**

4. Proposed approach

The objective of the proposed approach is to involve human perception during the design space exploration to create variant design alternatives. To achieve this, we introduced a psycho-physical distance metric which is extracted using human judgment about the design diversification. The steps for developing the psycho-physical distance metric for any given CAD model is introduced, which will be then utilized for exploring design variations.

4.1. Design parametrization and design space formulation

The decision on the selection of appropriate geometric parameters is critical for representing a parametric shape well. Literature comprises a substantial amount of work for the generation of a well-structured parametric CAD model [55, 56], which should aid the designer to create plausible/feasible design variations compared to a poorly organized one. It is hard to keep the original physical form for a model with a vast number of parameters during parametric modification. Designers mostly desire to preserve the common underlying structure of the model during modifications [2]. Cagan et al. [57] have described the design parametrization process as an iterative task, in which the final decision on the selection of suitable design parameters depends on the designer's understanding, performance objective and design's construction process.

In this work, we followed the parametrization strategy of Khan and Awan [1], in which important features are first parametrized with a large number of geometric parameters. After some trials, quixotic parameters, which might disrupt the underline structure of the model or might account less in the overall variation, are eliminated.

Each parameter in the model represents a dimension in the design space, ϕ. To determine the boundary of the design space, the range of each parameter is first set. These parametric ranges usually set tentatively based on the designer's understanding of approximate parametric ranges for creating feasible designs [2], design specifications and functional requirements given by the customer [57] while keeping the initial design at the center of design space. If no design specifications are given in the conceptual phase, the upper and the lower bounds of an initial design space can be set, respectively, as a certain percentage of increment and decrement in initial parameter values of the input design [1].

4.2. Design clustering

First, N design alternatives are generated via S-TLBO technique in a predefined design space. $X = [x_{m,1}, x_{m,2}, \dots, x_{m,n}]$ denote geometric parameters for the design with index m. $[x^l_{m,j}]$ and $[x^u_{m,j}]$, respectively, represents the lower and upper bounds of the j^{th} parameter for the design with index m. These designs are then utilized in the user study to acquire the dissimilarity responses between designs from the subjects. Note that a higher number of design alternatives should be created at this stage to achieve higher diversities between designs. This diversity can help accurately capture dissimilarity responses between designs and will also create relatively big training data that potentially aids in nonlinear regression results. The paired comparison can be one way to compare $\binom{N}{2} = \frac{N!}{2!(N-2)!}$ design pairs in this study. This is, however, practically impossible and can cause respondent fatigue when N is large. To overcome this issue, similar designs are clustered into groups and comparisons are done between cluster pairs rather than individual design comparison.

The design alternatives are clustered into K clusters using Ward's hierarchical clustering method [58]. It is expected that some geometric parameters account more in the model's visual shape variation compared to others. If design clustering is done based only on the geometric parameter values, visually unique designs may be in the same cluster because some parameters may have a higher impact on the visual appearance than others. For this reason, design clustering is performed based on a feature vector $\mathcal{F}$, which is shown in Equation 2 and comprises of not only n geometric parameters but also includes some geometry information of the model such as position of $(2n)$ sampled points ($S = [s_1, s_2, \dots s_{2n}]$) and $(2n)$ curvature values ($C = [c_1, c_2, \dots, c_{2n}]$) at these sampled points. Here, we assume that the CAD model is represented using curves, in which equal-distanced points are sampled along the curves' parametric length. For the model composed of multiple curves, $2n$ points are sampled on each curve. If there are no appropriate curves in the model, $\mathcal{F}$ contains only geometric parameters. The $\mathcal{F}$ is in the form of $N \times 5n$ matrix (see Equation 3) and illustrates a model represented using a single curve.

$$\mathcal{F} = \begin{bmatrix} (X)_{N\times n} & (S)_{N\times 2n} & (C)_{N\times 2n} \end{bmatrix} \tag{2}$$

$$(X)_{N\times n} = \begin{bmatrix} x_{1,1} & x_{1,2} & \dots & x_{1,n} \\ x_{2,1} & x_{2,2} & \dots & x_{2,n} \\ \vdots & \vdots & \vdots & \vdots \\ x_{N,1} & x_{N,2} & \dots & x_{N,n} \end{bmatrix} (S)_{N\times 2n} = \begin{bmatrix} s_{1,1} & s_{1,2} & \dots & s_{1,2n} \\ s_{2,1} & s_{2,2} & \dots & s_{2,2n} \\ \vdots & \vdots & \vdots & \vdots \\ s_{N,1} & s_{N,2} & \dots & s_{N,2n} \end{bmatrix}$$

$$(C)_{N\times 2n} = \begin{bmatrix} c_{1,1} & c_{1,2} & \dots & c_{1,2n} \\ c_{2,1} & c_{2,2} & \dots & c_{2,2n} \\ \vdots & \vdots & \vdots & \vdots \\ c_{N,1} & c_{N,2} & \dots & c_{N,2n} \end{bmatrix} \tag{3}$$

K clusters are formed based on $\mathcal{F}$ via Ward's clustering method. The optimal value for K is obtained using the Elbow partitioning method [59], which segments the designs into K clusters by minimizing the total intra-cluster variation or the total within sum of square (WSS). The total WSS measures the compactness of the clustering and should be kept as small as possible. The Elbow method takes WSS as a function of K. K is increased gradually and is set to a value so that further increment in K does not improve the total WSS.

4.2.1. Design sorting

The number of designs in each cluster can vary depending on the test model. This uneven size of each cluster can create confusion for the subjects in the user study. The size of the cluster pairs is equalized to the size of the smallest one of the two. This is done by removing designs from the cluster having a higher number of designs. The decision on which design to remove should be made in a systematic way. Randomly choosing a design and removing it from the cluster might result in removal of the most representative designs of the cluster. Therefore, a furthest-point-sorting technique is proposed to equalize the designs while ensuring the most representative designs of the cluster retain in the cluster.

Let D be the number of designs in the cluster k, which is sorted and inserted in a design set, R, using Algorithm 2. The most representative design is first found that has a minimum Euclidean distance to the centroid of the cluster E_k. The representative design is then removed from the cluster and inserted in R. Afterward, a design is selected from the cluster which maximizes the minimum Euclidean distance with the design(s) in R. Other designs are chosen in this manner and placed in R. When D designs are found, the algorithm stops.

Algorithm 2 The pseudo-code of furthest-point-sorting algorithm

1: Centroid of the cluster $E_k = \frac{\sum_{i=1}^{D} X_i}{D}$
2: Find the first representative design, $r_1 = min_{EuclideanDist}(E_C, X_{1,2,\dots,D} \in k)$
3: Place the first representative in set R ($R \leftarrow r_1$)
4: **for** $i = 2$ to D **do**
5: $\quad r_i = argmax_{(X)}\ mini_{EuclideanDist}(R, X_{1,2,\dots,D-(i-1)} \in k)$
6: $\quad R \leftarrow r_i$
7: **end for**

4.3. Extracting psycho-physical distance metric

A user study was designed that includes a survey consisting of $\binom{K}{2}$ cluster pairs to be rated for their dissimilarities by the subjects. The subjects ranked their perceptual judgment about the cluster dissimilarities using a seven-point Likert scale with anchor ranges from "Very Similar" (1) to "Very Dissimilar" (7). For the better estimation of perceptual dissimilarities between design clusters, it is required to have enough response data from the subjects. Therefore, Amazon Mechanical Turk (AMT) [60] platform was utilized. To ensure the reliability of data coming from subjects, different rules were considered. We hired subjects who were qualified as Masters by AMT. Note that AMT awards Master qualification to the subjects who demonstrate excellence across a wide range of tasks and AMT monitors their performance over time. Furthermore, 10% of the total cluster pairs were duplicated and were shuffled randomly in the study. To check the consistency of a subject's scores, a consistency metric is computed using Equation 4. Here, $\bar{r}_p$ represents the consistency metric for the $p^{th} subject$. m_1^s and m_2^s are, respectively, the scores given for the t^{th} pair and its duplicated pair. The subjects, whose consistency score were less than 90%, were excluded from the study. Furthermore, the subjects who performed the survey in less than 10 minutes were also disqualified.

$$\bar{r}_p = 100 - \left(100 \times \frac{\sum_{t=1}^{10\%\binom{k}{2}} r_t}{10\%\binom{k}{2}} \right) \tag{4}$$

with

$$r_t = \frac{|m_1^t - m_2^t|}{7} \tag{5}$$

Following instructions were given to the AMT subjects:

1. Carefully observe the designs in all views and then rank the dissimilarities between design clusters based on the given Likert scale.

2. The Likert scale has seven rank points from 1 to 7. The rank of 1 means that designs in two clusters are very similar and the rank of 7 means that cluster pairs are very dissimilar.
3. This part of the survey contains different cluster pairs sets, and you are required to rank the dissimilarities based on your personal opinion for each pair.
4. Make sure that you have carefully observed the designs in both clusters before assigning the final dissimilarity rank.
5. Make sure that you have spent more than 15 seconds on each pair.
6. We highly recommend you to take a small break after completing half of the survey to avoid fatigue.
7. This part of the survey will take a minimum of 10 minutes to complete.

Along with the above instructions, the reliability criterion was also mentioned to warn subjects to perform their task honestly. To motivate subjects, we provided a bonus of 10% of the original credit to the subjects who 100% satisfied the reliability criteria.

We divided the $\binom{K}{2}$ cluster pairs into two sets of surveys. The subjects were asked to complete the first part of the survey, and their reliability scores were then checked. If a subject passes our reliability criterion, the subject was allowed to conduct the second part of the survey. After excluding the results of disqualified subjects, we hired more subjects. The process was repeated until responses from 50 qualified subjects were obtained.

After acquiring the dissimilarity responses for the $\binom{K}{2}$ cluster pairs, the dataset is prepared to construct the relationship between the dissimilarity responses and the geometric parameters via the regression analyses. During the user study, the perceptual responses from the subjects are the differences between the appearances of the designs in the clusters, which are regarded as dissimilarity responses between the cluster pairs in the current study. Therefore, an average distance measure, shown in Equation 6, is utilized to measure the average of the difference between geometric parameters of the designs in the clusters that are being compared. Here, these average differences are the predictor or independent variables, and the averaged responses from all subjects for each cluster pair are the dependent variables for the regression analysis. The dataset is standardized by normalizing the dependent and independent variables between 0 and 1.

$$\Delta x_j = \frac{1}{D_p}\frac{1}{D_q}\sum_{p=1}^{D_p}\sum_{q=1}^{D_q}\|\overline{x}_{p,j} - \overline{x}_{q,j}\| \tag{6}$$

Here, Δx_j is the average difference between the j^{th} parameter of the designs in the paired clusters. p and q, respectively, represent the indices of the designs in the cluster and its pair. In addition, D_p and D_q are the number of designs in the cluster and its pair, respectively. $\overline{x}_{p,j}$ and $\overline{x}_{q,j}$ are the scaled parameter values for design p and q. Now the dataset consists of a vector of independent variables ($\Delta X = [\Delta x_1, \Delta x_2, \ldots, \Delta x_n]$) and a dependent variable Y, which is the scaled average value of dissimilarity ranks in seven-point Likert scale. To construct a numerical relationship between these variables, we utilized a weighted distance metric shown in equation 7, where $W = [w_1, w_2, \ldots, w_n]$ are the weighted coefficients and $f(\Delta X, W)$ is the metamathematical model that provides the fitted or estimated dissimilarity values for each cluster pair. The coefficients in Equation 7 are estimated via regression analysis to extract a psycho-physical distance metric.

$$f(\Delta X, W) = \sqrt{\sum_{j=1}^{n} w_j \times \|\Delta x_j\|^2} \tag{7}$$

The general form of the regression model is represented as $Y = f(\Delta X, W) + \varepsilon$ in which the response Y consists of two parts. The systematic part $f(\Delta X, W)$, which contains the unknown weight coefficients W that need to be estimated, and the random error part ε, which subjects to the normal distribution and independent from predictors.

To estimate the weight coefficients in a nonlinear regression function, a least-squares technique [61] is employed as shown in equation 8. The nonlinear weight estimation is an optimization problem, in which the optimization technique tries to find the values of coefficients W that minimizes the objective function $S(W)$ between the observed response Y from subjects and the predictions of the model $f(\Delta X, W)$.

$$S(W) = \sum_{l=1}^{\binom{K}{2}} (Y^l - f(\Delta X^l, W))^2 \tag{8}$$

Here, Y^l and ΔX^l denotes the l^{th} sample data of dependent and independent variable, respectively, and each l corresponds to one of $\binom{K}{2}$ cluster pairs. The minimization of least-squares criterion is often referred to as minimizing residual sums of squares (RSS) with respect to W. As $S(W)$ is nonlinear and has a various local minimum, it might be advantageous to use meta-heuristic techniques like TLBO instead of classical methods such as Gauss-Newton method, which is a simple iterative gradient descent optimization method. The latter approach requires good starting values for the unknown coefficients to converge to global optima, which is critical if n is large like in this work. Therefore, in this study, the regression analyses are performed via TLBO following the similar methodology as employed in [62, 63], which utilized particle swarm optimization and genetic algorithms to estimate the coefficients of any nonlinear mathematical model. The advantages of TLBO over techniques like genetic algorithm and particle swarm optimization is its simplicity and no requirement of algorithmic tuning parameters.

After estimating the weight coefficients, the psycho-physical distance metric (H_{pq}) is formalized as in Equation 9 and the space-filling design alternatives are created using the psycho-physical distance-based potential energy $U(W)$, shown in Equation 10.

$$H_{pq} = \sqrt{\sum_{j=1}^{n} w_j \times (\overline{x}_{p,j} - \overline{x}_{q,j})^2} \tag{9}$$

and

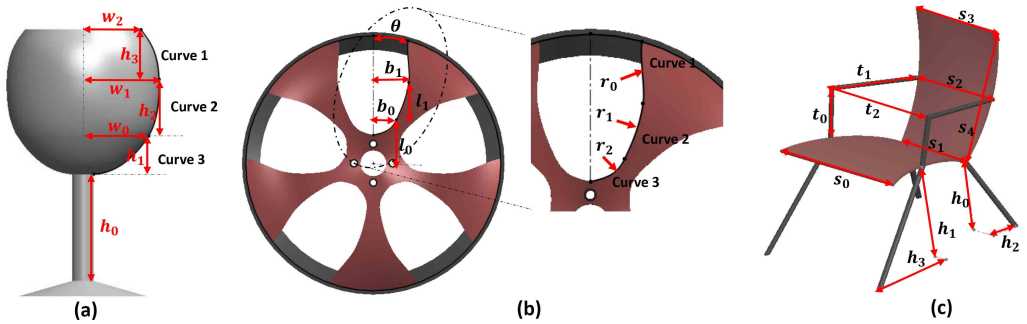

Figure 3: CAD models for a wine glass (a), a wheel rim (b) and a chair (c) with their geometric parameters.

$$U(W) = \sum_{p=1}^{N-1} \sum_{q=p+1}^{N} \frac{1}{H_{pq}^2} \tag{10}$$

Here, $\overline{x}_{p,j}$ and $\overline{x}_{q,j}$ are the scaled parameter values for design p and q, respectively.

5. Results and Discussion

In this section, three different CAD models will be first introduced that are used in this study's experiments. Reliability of the mathematical model established to learn the weights of the geometric parameters is then discussed. Afterward, the proposed psycho-physical distance metric is integrated into the sampling process of S-TLBO for the generation of user-driven variant designs. Finally, the performance of psycho-physical and Euclidean distance metrics are compared via three user studies for the test models.

5.1. CAD models

Three CAD models, a wine glass, a wheel rim, and a chair, are introduced to validate the performance of the proposed approach and are shown in Figure 3. These models are selected based on their aesthetic importance. For instance, a wine glass defines the elegance of the wine drinker; an attractive wheel rim can make the automobile graceful and elegant furniture can enhance the ambiance of a place. These models are parameterized to achieve higher design variations while keeping their underlying form same. 3D surfaces of the wine glass model are created by interpolating Coons patches between Bezier curves and the geometric parameters are defined on these curves. The chair and wheel rim models are the 3D solid models. Seven geometric parameters of the wine glass model are shown in Figure 3 (a). $h_1/h_2/h_3$ and $w_1/w_2/w_3$ denote the lengths and widths, respectively, for the first/second/third curve and h_0 is the vertical length of glass's stem. The spokes of the wheel rim are also created using three cubic Bezier curves (see Figure 4 (d)). b_0/b_1 and l_0/l_1 denote the width and length of the first/second curve, respectively. θ controls the position of the third curve on the outer circle of the wheel rim. r_0, r_1 and r_2 represents the minimum radii of the curvature for the first, second and third curves, respectively.

The chair model is represented using 12 geometric parameters, as shown in Figure 3 (c). s_0 and s_1 are the widths for the seat. s_2/s_3 and s_4 are the width and length of the backrest of the chair, respectively. t_0 and t_1 denote, respectively, the vertical and horizontal lengths of the armrests. t_2 is the spacing between armrests. h_0/h_1 denotes the highest and h_2/h_3 represents the horizontal positioning of the back and front legs of the chair, respectively. The parameter ranges for these models are given in Table 1. The CAD model modifications of the glass and rim were performed using the technique proposed by Khan et al. [64].

Table 1: Parameter ranges of the wine glass, wheel rim, and chair models.

Parametric Ranges			
Wine Glass Model			
$6 \le h_0 \le 13$	$18 \le h_1 \le 23$	$26 \le h_2 \le 31$	$35 \le h_3 \le 40$
$3.5 \le w_0 \le 12$	$7.5 \le w_1 \le 12$	$6.5 \le w_2 \le 12$	
Wheel Rim Model			
$12 \le l_0 \le 27$	$28 \le l_1 \le 40$	$5 \le b_0 \le 10$	$0.05 \le b_1 \le 21$
$3.5 \le \theta \le 30$	$0 \le r_0 \le 1$	$0 \le r_1 \le 5$	$0 \le r_2 \le 5$
Chair Model			
$23 \le t_0 \le 33$	$13 \le t_1 \le 64$	$20 \le t_2 \le 40$	$30 \le s_0 \le 75$
$25 \le s_1 \le 60$	$25 \le s_2 \le 70$	$25 \le s_3 \le 80$	$70 \le s_4 \le 95$
$22 \le h_0 \le 30$	$2 \le h_1 \le 22$	$26 \le h_2 \le 36$	$20 \le h_3 \le 48$

5.2. Psycho-physical distance metric

Fifty design alternatives for the wine glass, wheel rim and chair models are generated to learn the psycho-physical distance metric, which is shown in Figure 4, 5 and 6, respectively. These initial models are created utilizing S-TLBO under the setting of $s = 30$ and $\alpha = 5$. Recall that s denotes the size of each sub-population, and α adjusts the degree of non-collapsing between designs. According to the experiments, S-TLBO converges after 80, 110 and 150 iterations for the wine glass, wheel rim, and chair models, respectively, as shown in Figure 4, 5 and 6. The plots for $U(T)$ versus the number of iterations can be seen in Figure 7. No improvements were observed in the cost function $U(T)$ after some iterations.

The results for the design clustering are represented in the dendrograms, as shown in Figure 8. Recall that the decision on the selection for an optimal value of K is made using the Elbow partitioning method. Figure 9 (a), (b) and (c) shows the plots for the number of clusters versus total within sum of square (WSS)

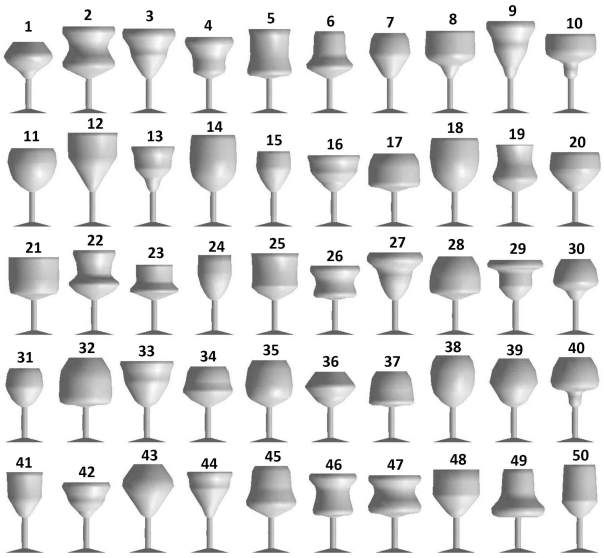

Figure 4: Design alternatives generated for the wine glass model.

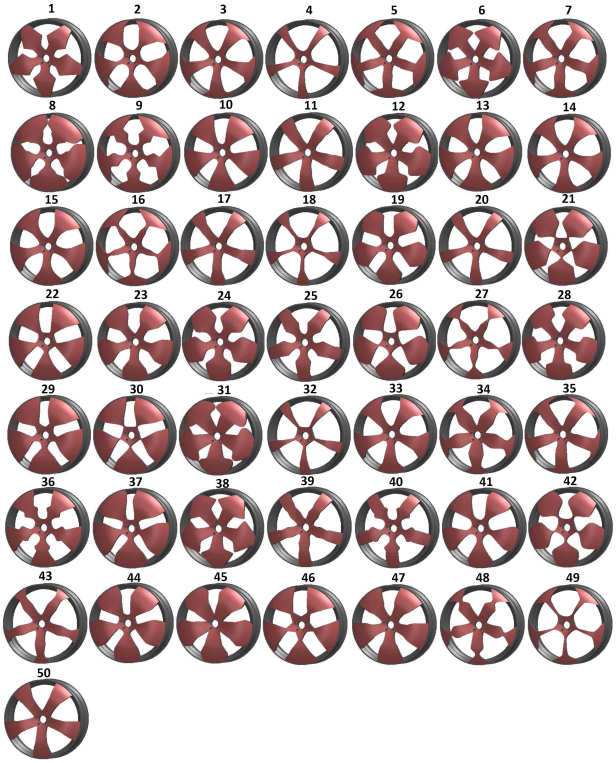

Figure 5: Design alternatives generated for the wheel rim model.

for the wine glass, wheel rim and chair models, respectively. According to the plots, K is selected as 11, 12 and 15, respectively, for the glass, rim and chair models. After clustering, the designs in each cluster were sorted based on the furthest-point-sorting algorithm. The sorting results of all three models are shown in Table 2. Afterward, surveys were conducted to learn the perceptual dissimilarity responses between 55, 66 and 105 cluster pairs for the glass, rim, and chair models, respectively.

Three different surveys were created for three CAD models. The surveys for the glass and rim model were divided into two

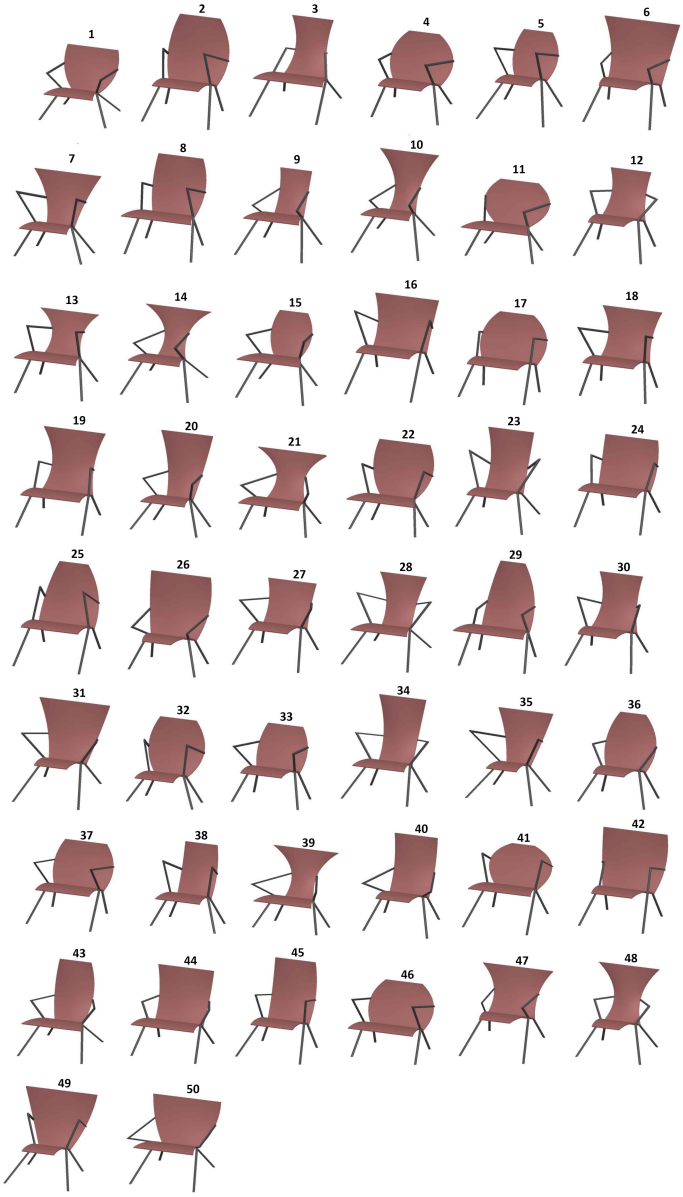

Figure 6: Design alternatives generated for the chair model.

Table 2: Sorting for the glass, rim and chair designs in their clusters

Clusters	Wine Glass	Wheel Rim	Chair
1	17, 21, 32, 28	14, 2, 46, 15, 23	8, 25, 29, 2
2	34, 25, 37, 35, 45	16, 48, 49, 43, 27	18, 33, 13
3	19, 46, 49, 6, 23, 22, 5	20, 32, 18, 50, 11, 17	46, 4, 37
4	47, 26, 2	7, 35, 34, 45, 5, 3	17, 41
5	4, 29	4	44, 50, 42, 16, 24
6	9, 3, 27, 42, 44, 13	19, 26, 42, 25, 41	28, 19, 3, 43
7	15, 41, 50, 7, 24, 31	8, 9	31, 6, 49, 47
8	14, 38, 11, 18	40, 36	26, 40
9	20, 39, 33, 48, 16, 12	6, 28, 31, 38, 12	30, 48, 27, 12, 23
10	43, 36, 1	33, 22, 10, 44, 13, 29	1, 11
11	40, 8, 10, 30	1, 39, 24, 47	10, 14
12	1, 39, 24, 47	37, 21, 30	9, 5, 15
13	-	-	7, 21, 35, 39
14	-	-	45, 20, 34
15	-	-	32, 22, 36, 38

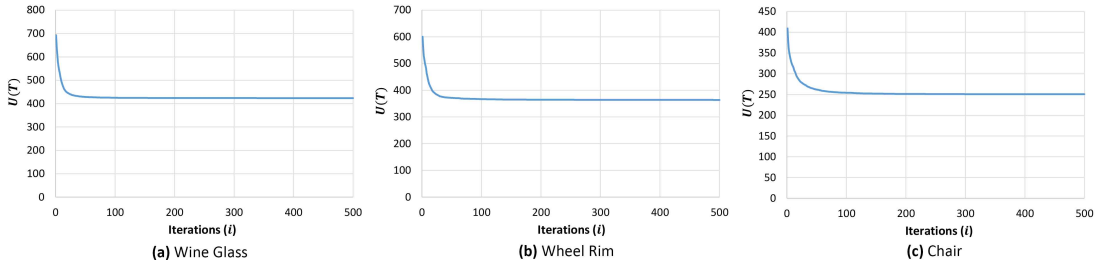

Figure 7: The plots showing the cost $U(T)$ versus number of S-TLBO iterations for the models, respectively, in Figure (a) 4, (b) 5, and (c) 6.

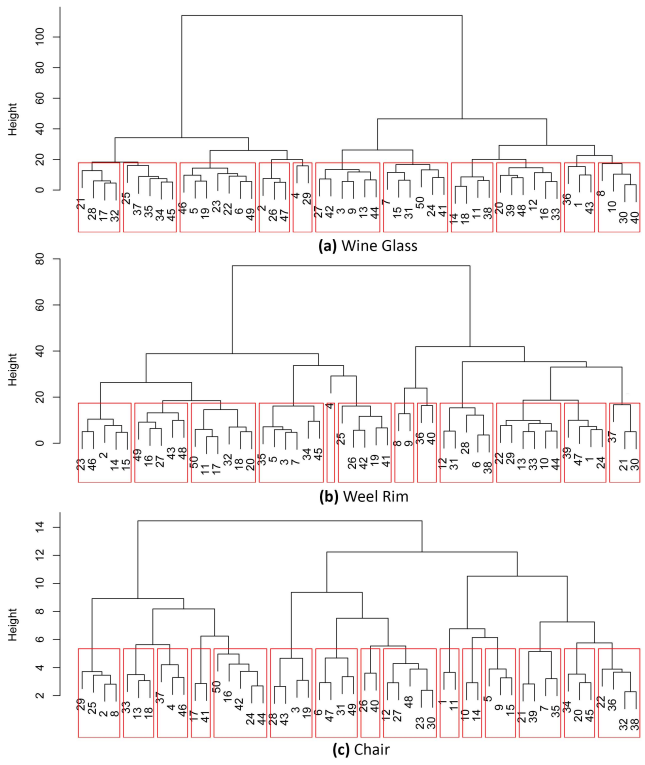

Figure 8: Dendrogram for the design clustering of the wine glass (a), wheel rim (b) and chair (c) design alternatives.

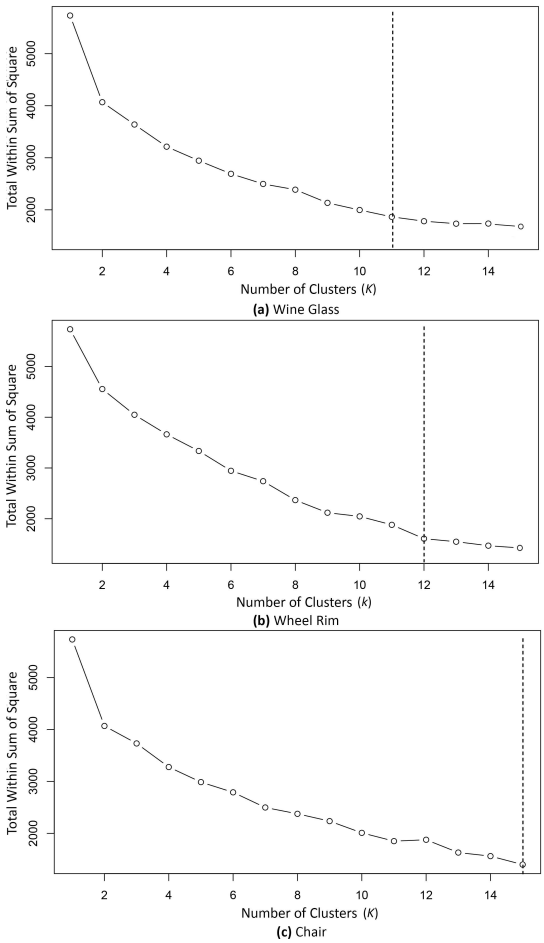

Figure 9: Plots for number of clusters vs. total within sum of square (WSS) for the wine glass (a), wheel rim (b) and chair (c) models, respectively.

parts, and the survey for the chair model was divided into four parts due to its high number of cluster pairs and to achieve reliable results from the subjects. The survey for each model was conducted with 50 different subjects selected from the AMT. As mentioned in the section 4.3, the subjects having unreliable results were eliminated. The elimination rate, which is the percentage rate of the number of subjects got rejected over the total number of subject that participated, for the rim, glass and chair surveys was 36.7%, 44.4%, and 23%, respectively. The nonlinear regression was performed, as described in section 4.3, to estimate the weights in the psycho-physical distance metric (see Equation 9). Table 3 includes the RSS values and computed weights corresponding to each geometric parameter for the three CAD models. Equation 11, 12 and 13 are the psychophysical distance between design p and q of wine glass, wheel rim and chair models, respectively. Later, the space-filling design alternatives for these models can be created using psychophysical distance-based potential energy $U(W)$ in Equation 10.

$$\begin{aligned} H_{pq} = {} & 0.2306 \times (h_{p,0} - h_{q,0})^2 + 0.3582 \times (w_{p,0} - w_{q,0})^2 + \\ & 0.2174 \times (h_{p,1} - h_{q,1})^2 + 0.2961 \times (w_{p,1} - w_{q,1})^2 + \\ & 0.1884 \times (h_{p,2} - h_{q,2})^2 + 0.6310 \times (w_{p,2} - w_{q,2})^2 + \\ & 0.0735 \times (h_{p,3} - h_{q,3})^2 \end{aligned} \tag{11}$$

$$\begin{aligned} H_{pq} = {} & 0.3374 \times (b_{p,0} - b_{q,0})^2 + 0.1147 \times (l_{p,0} - l_{q,0})^2 + \\ & 0.9874 \times (b_{p,1} - b_{q,q})^2 + 2.60E-5 \times (l_{p,1} - l_{q,1})^2 + \\ & 0.2913 \times (\theta_p - \theta_q)^2 + 0.1819 \times (r_{p,0} - r_{q,0})^2 + \\ & 0.8321 \times (r_{p,1} - r_{q,1})^2 + 0.0841 \times (r_{p,2} - r_{q,2})^2 \end{aligned} \tag{12}$$

Table 3: Weights for the geometric parameters coefficient of psycho-physical distance metric in Equation 9 for the three test models.

Weights	Test Models		
	Wine Glass	Wheel Rim	Chair
W_1	0.2306	0.3374	0.1574
W_2	0.3582	0.1147	0.0215
W_3	0.2174	0.9874	0.5351
W_4	0.2961	2.60E-5	0.4394
W_5	0.1884	0.2913	0.0619
W_6	0.6310	0.1819	0.0201
W_7	0.0735	0.8321	0.0495
W_8	-	0.0841	0.0596
W_9	-	-	0.2585
W_{10}	-	-	0.1228
W_{11}	-	-	0.0727
W_{12}	-	-	0.3521
RSS	0.3119	0.6582	0.5342

$$
\begin{aligned}
H_{pq} = {} & 0.1574 \times (s_{p,0} - s_{q,0})^2 + 0.0215 \times (s_{p,1} - s_{q,1})^2 + \\
& 0.5351 \times (s_{p,2} - s_{q,2})^2 + 0.4394 \times (s_{p,3} - s_{q,3})^2 + \\
& 0.0619 \times (s_{p,4} - s_{q,4})^2 + 0.0201 \times (h_{p,0} - h_{q,0})^2 + \\
& 0.0495 \times (h_{p,1} - h_{q,1})^2 + 0.0596 \times (h_{p,2} - h_{2,q})^2 + \\
& 0.2585 \times (h_{p,3} - h_{q,3})^2 + 0.1228 \times (t_{p,0} - t_{q,0})^2 + \\
& 0.0727 \times (t_{p,1} - t_{q,1})^2 + 0.3521 \times (t_{p,2} - t_{q,2})^2
\end{aligned} \tag{13}
$$

5.2.1. Cross-validation

We utilized k-fold cross-validation [65] to validate the accuracy of the mathematical model of the psycho-physical distance metric computed. The dataset was partitioned into k_c groups/folds, and one fold was used for validation/test and the remaining $k_c - 1$ groups were used as the training dataset to calculate the psycho-physical distance metric. The dissimilarity responses for the validation dataset were then predicted using the psycho-physical distance metric obtained from the training dataset. The root-mean-square-error (RMSE) was calculated using Equation 14 for the actual and predicted response values.

$$
RMSE = \sqrt{\frac{\sum_{i=1}^{g} (Y_i - Y_i')^2}{g}} \tag{14}
$$

Here, Y_i and Y_i' are, respectively, the actual and predicted response values for the validation dataset consisting of a g number of observations. The cross-validation process was repeated k_c-times while taking each k_c fold as a validation dataset. After obtaining k_c results of W and RMSE from the folds, the final estimation of W and values of RMSE were calculated by averaging all k_c weight coefficients and RMSE values.

In this work, k_c was set to 5 for the glass and chair models, and it was set to 6 for the rim model. The mean RMSE of the glass, rim and chair models is 0.0981, 0.0786 and 0.0694, respectively. The small RMSE values indicate that our psycho-physical distance metric can reliably involve the human perception about the design dissimilarities.

Furthermore, to validate the performance of the proposed nonlinear regression technique, we have compared its RMSE values with those obtained from the linear regression and Generalized Regression Neural Networks (GRNN) [66]. Table 4 shows the RMSE values for the methods. It can be observed that the RMSE values of the nonlinear regression are less than those of the linear regression and GRNN for the rim and chair models, whereas the values for the methods are approximately same for the glass model. Therefore, the nonlinear regression was chosen in this work.

Table 4: Comparison between linear regression, nonlinear regression and GRNN for glass, chair and rim models

Methods	Root Mean Square Error		
	Glass	Rim	Chair
Linear Regression	0.0937	0.1363	0.0829
Proposed Nonlinear Regression	0.0981	0.0786	0.0694
GRNN	0.0919	0.1631	0.1155

5.3. Comparative study

The space-filling quality of the designs generated based on Euclidean and psycho-physical distances are investigated in this section. An additional user study was conducted to compare the space-filling performance of the Euclidean and psycho-physical distance-based design exploration. If the space-filling potential energy of the design alternatives generated using psycho-physical distance-based design exploration is less then that of Euclidean distance-based design exploration (i.e., S-TLBO), the designs obtained from the former metric have better design diversification. Fifteen designs were generated for the glass, chair, and rim models. Dissimilarity ranks between the $\binom{15}{2}$ design pairs of the Euclidean and psycho-physical distance-based exploration were learned in this user study. Similar to the previous user study, the seven-point Likert scale was also utilized here, with anchor ranging from 1 ("Very Similar") to 7 ("Very Dissimilar"). The design pairs from both techniques were shuffled with the duplication of 10% of total designs to measure the reliability of the subjects' response. In this study, 50 subjects were involved, who had no knowledge of the techniques used to sample the designs. Here, the elimination rate of the subjects was 16.6%, 24% and 10.7% for the rim, glass and chair models. After obtaining the dissimilarity ranks, the space-filling for the designs obtained from both techniques was calculated with Equation 15 by using the subjects' ranks as distances between the designs. In Equation 15, R_{pq} denotes the dissimilarity rank between designs p and q given by the subject.

$$
U = \sum_{p=1}^{N-1} \sum_{q=p+1}^{N} \frac{1}{R_{pq}} \tag{15}
$$

Figure 10 (a), (b) and (c) shows the designs obtained, respectively, for the wine glass, wheel rim, and chair models using S-TLBO (which uses Euclidian distance metric for design exploration) and the proposed approach (in which designs are explored using psycho-physical distance metric). The designs

generated by these techniques were compared in the comparative study. For the proposed approach, the design exploration process stopped at the 220^{th}, 150^{th} and 250^{th} iterations for the wine glass, wheel rim and chair models, respectively (see Figure 11). The plots in Figure 12 shows the space-filling values for the design alternatives in Figure 10, which were calculated with the dissimilarity ranks (R_{pq}) in Equation 15. In these plots, underlined numbers are the subjects who responded that S-TLBO generated better space-filling designs than proposed approach. In the case of the glass, wheel rim and chair models, according to 38, 40 and 49 subjects among 50, respectively, space-filling for the designs generated using proposed technique was better than that of S-TLBO. From the results of the user study, it can be concluded that the designs obtained using psycho-physical distance-based exploration had more visual variations compared to those generated using S-TLBO.

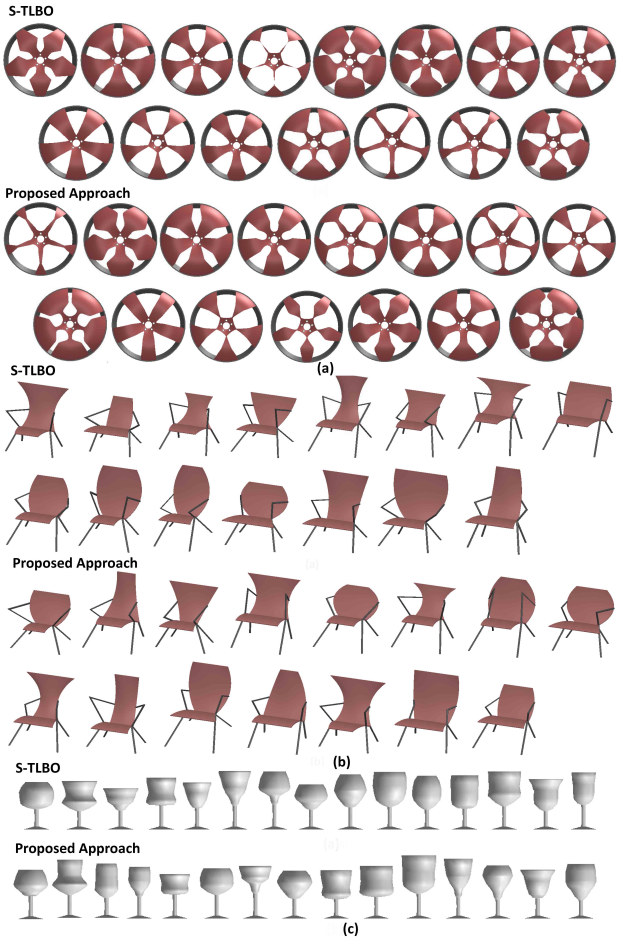

Figure 10: Design alternatives of the wheel rim (a), chair (b) and wine glass (c) models generated via Euclidean and psycho-physical distance-based S-TLBO.

We also conducted a statistical test, called *Friedman Test*, to check whether there is a significant difference between the space-filling of the designs generated using Euclidean and psycho-physical distance-based S-TLBO. The Friedman test is a nonparametric statistical test [67], and one of its primary merits being that it does not get affected by the dataset distribution compare to the other statistical test like *t-test*, which is appropriate only if the dataset is normally distributed. In the Friedman test, two hypotheses the null hypothesis H_0 and alternative hypothesis H_1 are defined. H_0 states that there is no significant difference between space-filling obtained for the designs, H_1 states that there is a significant difference between the two approaches. In this test, a χ^2 and p-values provide information about whether a statistical hypothesis test is true. If the p-value is less than 0.05 and the value of χ^2 is greater than the χ^2-critical, there is strong evidence against H_0. Table 5 provides the results of the Friedman Test for all three test models. For the glass, rim and chair models, the p-values are less than 0.05 and χ^2 values are greater than χ^2-critical. These results showed strong evidence against H_0, thereby indicating a significant difference between space-filling from the two sampling techniques.

Table 5: Statistical and Friedman test results for the design alternatives used in the comparative survey.

	Wine Glass	Wheel Rim	Chair
p-value	0.003283	3.43E-5	1.14E-11
χ^2	8.6429	17.163	46.08
χ^2-critical	3.84		
μ	24.24	26.16	26.03
σ	4.95	7.62	4.83
$Skewness$	0.75	1.33	0.55

6. Conclusions and future works

This paper proposed a psycho-physical generative design approach for design exploration for CAD models. The proposed approach involves the users' psychological judgment about the design variations in the design space exploration via a psycho-physical distance metric. To extract this metric, a user study was conducted, in which pair comparison was utilized to ask subjects to rank their perceptual response about the shape dissimilarities between the design clusters. The nonlinear regression analysis was performed using the teaching-learning-based optimization technique to link the subjects' dissimilarity responses with the geometric parameters, and a psycho-physical distance metric was obtained. Finally, a comparative survey was conducted to compare the performance of the Euclidean and psycho-physical distance-based S-TLBO regarding creating variant design alternatives.

As a future work, we would like to develop a psycho-physical distance based interactive technique to make users involved in the design exploration process. We are also planning to establish a large dataset for CAD models and construct a psycho-physical distance metric for each model. Finally, a similar methodology will be utilized to create a user-centered generative design technique for parametric exploration of 3D animated characters.

[1] S. Khan, M. J. Awan, A generative design technique for exploring shape variations, Advanced Engineering Informatics 38 (2018) 712–724.

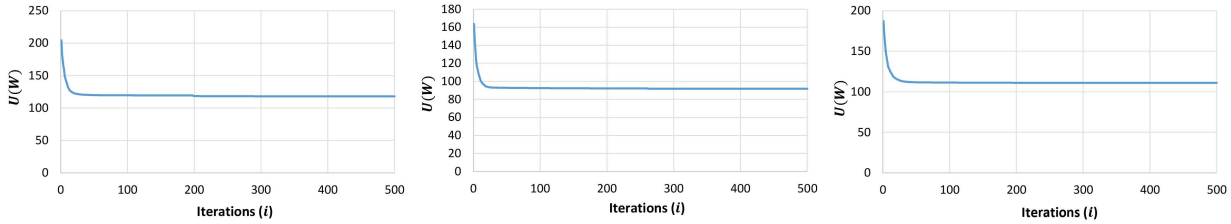

Figure 11: (a), (b) and (c) are the plots showing the cost value $U(W)$ versus number of iterations for the models in Figure 10 (a), (b), and (c), respectively, generated using the psycho-physical distance-based S-TLBO.

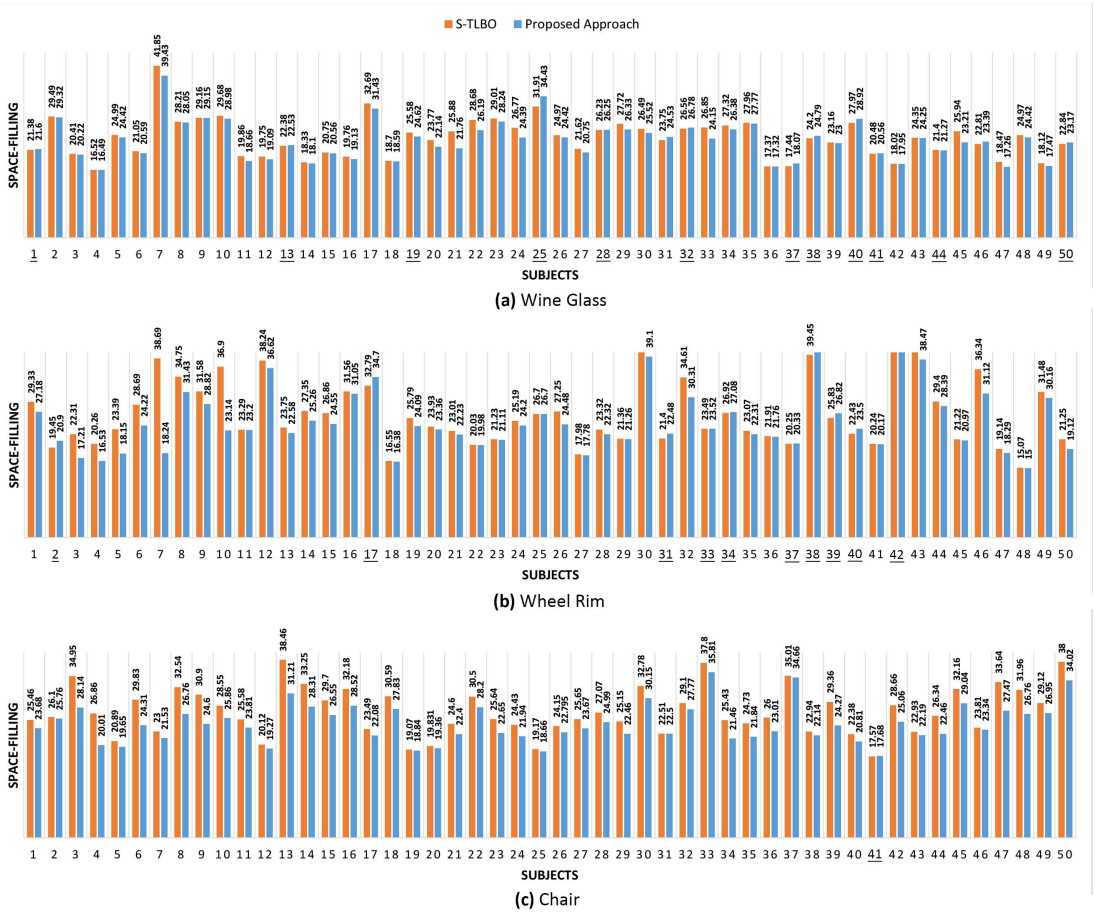

Figure 12: Space-filling values for the 50 subjects participated in the comparative survey. The space-filling values are obtained using Equation 15 for the glass (a) wheel rim (b) and chair (c) alternatives in Figure 10 generated via Euclidean and psycho-physical distance-based S-TLBO.

[2] S. Krish, A practical generative design method, Computer-Aided Design 43 (1) (2011) 88–100.

[3] Autodesk, Project fractal (2018).
URL `https://home.fractal.live/`

[4] S. Khan, E. Gunpinar, Sampling cad models via an extended teaching–learning-based optimization technique, Computer-Aided Design 100 (2018) 52–67.

[5] R. V. Rao, V. J. Savsani, D. Vakharia, Teaching–learning-based optimization: a novel method for constrained mechanical design optimization problems, Computer-Aided Design 43 (3) (2011) 303–315.

[6] E. Gunpinar, U. C. Coskun, M. Ozsipahi, S. Gunpinar, A generative design and drag coefficient prediction system for sedan car side silhouettes based on computational fluid dynamics, Computer-Aided Design 111 (2019) 65–79.

[7] S. V. Patel, M. K. Tam, C. T. Mueller, 3dj: An analytical and generative design system for synthesizing high-performance textures from 3d scans, in: Design Computing and Cognition'16, Springer, 2017, pp. 477–494.

[8] R. H. Kazi, T. Grossman, H. Cheong, A. Hashemi, G. Fitzmaurice, Dreamsketch: Early stage 3d design explorations with sketching and generative design, in: Proceedings of the 30th Annual ACM Symposium on User

Interface Software and Technology, ACM, 2017, pp. 401–414.

[9] E. Gunpinar, S. Gunpinar, A shape sampling technique via particle tracing for cad models, Graphical Models 96 (2018) 11–29.

[10] G. S. Hornby, Functional scalability through generative representations: the evolution of table designs, Environment and Planning B: Planning and Design 31 (4) (2004) 569–587.

[11] M. Barros, J. P. Duarte, B. Chaparro, Integrated generative design tools for the mass customization of furniture, in: Design Computing and Cognition'12, Springer, 2014, pp. 285–300.

[12] S. Khan, E. Gunpinar, M. Moriguchi, Customer-centered design sampling for cad products using spatial simulated annealing, in: Proceedings of CAD17, Okayama, Japan, 2017, pp. 100–103.

[13] K. Shea, R. Aish, M. Gourtovaia, Towards integrated performance-driven generative design tools, Automation in Construction 14 (2) (2005) 253–264.

[14] M. Turrin, P. Von Buelow, R. Stouffs, Design explorations of performance driven geometry in architectural design using parametric modeling and genetic algorithms, Advanced Engineering Informatics 25 (4) (2011) 656–675.

[15] P. Janssen, Dexen: A scalable and extensible platform for experimenting with population-based design exploration algorithms, AI EDAM 29 (4) (2015) 443–455.

[16] L. Troiano, C. Birtolo, Genetic algorithms supporting generative design of user interfaces: examples, Information Sciences 259 (2014) 433–451.

[17] J. J. L. Kitchley, A. Srivathsan, Generative methods and the design process: A design tool for conceptual settlement planning, Applied Soft Computing 14 (2014) 634–652.

[18] L. Caldas, Generation of energy-efficient architecture solutions applying gene_arch: An evolution-based generative design system, Advanced Engineering Informatics 22 (1) (2008) 59–70.

[19] G. Stiny, Introduction to shape and shape grammars, Environment and planning B: planning and design 7 (3) (1980) 343–351.

[20] P. Prusinkiewicz, M. Shirmohammadi, F. Samavati, L-systems in geometric modeling, International Journal of Foundations of Computer Science 23 (01) (2012) 133–146.

[21] E. Kalogerakis, S. Chaudhuri, D. Koller, V. Koltun, A probabilistic model for component-based shape synthesis, ACM Transactions on Graphics (TOG) 31 (4) (2012) 55.

[22] S. Chaudhuri, E. Kalogerakis, S. Giguere, T. Funkhouser, Attribit: content creation with semantic attributes, in: Proceedings of the 26th annual ACM symposium on User interface software and technology, ACM, 2013, pp. 193–202.

[23] V. Granadeiro, L. Pina, J. P. Duarte, J. R. Correia, V. M. Leal, A general indirect representation for optimization of generative design systems by genetic algorithms: Application to a shape grammar-based design system, Automation in Construction 35 (2013) 374–382.

[24] J. P. McCormack, J. Cagan, Designing inner hood panels through a shape grammar based framework, Ai Edam 16 (4) (2002) 273–290.

[25] J. Cui, M.-X. Tang, Integrating shape grammars into a generative system for zhuang ethnic embroidery design exploration, Computer-Aided Design 45 (3) (2013) 591–604.

[26] L. Zimmermann, T. Chen, K. Shea, A 3d, performance-driven generative design framework: automating the link from a 3d spatial grammar interpreter to structural finite element analysis and stochastic optimization, AI EDAM 32 (2) (2018) 189–199.

[27] V. Singh, N. Gu, Towards an integrated generative design framework, Design Studies 33 (2) (2012) 185–207.

[28] W. Palubicki, K. Horel, S. Longay, A. Runions, B. Lane, R. Měch, P. Prusinkiewicz, Self-organizing tree models for image synthesis, ACM Transactions on Graphics (TOG) 28 (3) (2009) 58.

[29] J.-E. Marvie, J. Perret, K. Bouatouch, The fl-system: a functional l-system for procedural geometric modeling, The Visual Computer 21 (5) (2005) 329–339.

[30] K. M. Dogan, H. Suzuki, E. Gunpinar, M.-S. Kim, A generative sampling system for profile designs with shape constraints and user evaluation, Computer-Aided Design 111 (2019) 93–112.

[31] K. Dev, M. Lau, L. Liu, A perceptual aesthetics measure for 3d shapes, arXiv preprint arXiv:1608.04953.

[32] T. Liu, A. Hertzmann, W. Li, T. Funkhouser, Style compatibility for 3d furniture models, ACM Transactions on Graphics (TOG) 34 (4) (2015) 85.

[33] I. Lim, A. Gehre, L. Kobbelt, Identifying style of 3d shapes using deep metric learning, in: Computer Graphics Forum, Vol. 35, Wiley Online Library, 2016, pp. 207–215.

[34] A. Secord, J. Lu, A. Finkelstein, M. Singh, A. Nealen, Perceptual models of viewpoint preference, ACM Transactions on Graphics (TOG) 30 (5) (2011) 109.

[35] X. Zhang, X. Le, A. Panotopoulou, E. Whiting, C. C. Wang, Perceptual models of preference in 3d printing direction, ACM Transactions on Graphics (TOG) 34 (6) (2015) 215.

[36] S. Hoshyari, E. A. Dominici, A. Sheffer, N. Carr, Z. Wang, D. Ceylan, I. Shen, et al., Perception-driven semi-structured boundary vectorization, ACM Transactions on Graphics (TOG) 37 (4) (2018) 118.

[37] I. Tseng, J. Cagan, K. Kotovsky, Concurrent optimization of computationally learned stylistic form and functional goals, Journal of Mechanical Design 134 (11) (2012) 111006.

[38] I. Tseng, J. Cagan, K. Kotovsky, M. Wood, Form function fidelity, Journal of Mechanical Design 135 (1) (2013) 011006.

[39] H.-Y. Chen, Y.-M. Chang, Extraction of product form features critical to determining consumers perceptions of product image using a numerical definition-based systematic approach, International Journal of Industrial Ergonomics 39 (1) (2009) 133–145.

[40] L. Lin, M.-Q. Yang, J. Li, Y. Wang, A systematic approach for deducing multi-dimensional modeling features design rules based on user-oriented experiments, International Journal of Industrial Ergonomics 42 (4) (2012) 347–358.

[41] K. M. Dogan, E. Gunpinar, Learning yacht hull adjectives and their relationship with hull surface geometry using gmdh-type neural networks for human oriented smart design, Ocean Engineering 145 (2017) 215–229.

[42] M. P. Mata, S. Ahmed-Kristensen, P. B. Brockhoff, H. Yanagisawa, Investigating the influence of product perception and geometric features, Research in Engineering Design 28 (3) (2017) 357–379.

[43] J. C. Kelly, P. Maheut, J.-F. Petiot, P. Y. Papalambros, Incorporating user shape preference in engineering design optimisation, Journal of Engineering Design 22 (9) (2011) 627–650.

[44] C. Villa, R. Labayrade, Solving complex design problems through multiobjective optimisation taking into account judgements of users, Research in Engineering Design 25 (3) (2014) 223–239.

[45] G. J. Barnum, C. A. Mattson, A computationally assisted methodology for preference-guided conceptual design, Journal of mechanical design 132 (12) (2010) 121003.

[46] S. Orsborn, J. Cagan, P. Boatwright, Quantifying aesthetic form preference in a utility function, Journal of Mechanical Design 131 (6) (2009) 061001.

[47] E. Poirson, J.-F. Petiot, L. Boivin, D. Blumenthal, Eliciting user perceptions using assessment tests based on an interactive genetic algorithm, Journal of Mechanical Design 135 (3) (2013) 031004.

[48] Z. Gu, M. X. Tang, J. H. Frazer, Capturing aesthetic intention during interactive evolution, Computer-Aided Design 38 (3) (2006) 224–237.

[49] F. Fuerle, J. Sienz, Formulation of the audze–eglais uniform latin hypercube design of experiments for constrained design spaces, Advances in Engineering Software 42 (9) (2011) 680–689.

[50] T. M. Cioppa, T. W. Lucas, Efficient nearly orthogonal and space-filling latin hypercubes, Technometrics 49 (1) (2007) 45–55.

[51] M. W. Trosset, Approximate maximin distance designs, in: Proceedings of the Section on Physical and Engineering Sciences, 1999, pp. 223–227.

[52] E. Stinstra, D. den Hertog, P. Stehouwer, A. Vestjens, Constrained maximin designs for computer experiments, Technometrics 45 (4) (2003) 340–346.

[53] D. Draguljić, T. J. Santner, A. M. Dean, Noncollapsing space-filling designs for bounded nonrectangular regions, Technometrics 54 (2) (2012) 169–178.

[54] P. Audze, V. Eglais, New approach for planning out of experiments, Problems of dynamics and strengths 35 (1977) 104–107.

[55] J. D. Camba, M. Contero, P. Company, Parametric cad modeling: An analysis of strategies for design reusability, Computer-Aided Design 74 (2016) 18–31.

[56] C. M. Hoffmann, K.-J. Kim, Towards valid parametric cad models, Computer-Aided Design 33 (1) (2001) 81–90.

[57] J. Cagan, M. I. Campbell, S. Finger, T. Tomiyama, A framework for computational design synthesis: model and applications, Journal of Computing and Information Science in Engineering 5 (3) (2005) 171–181.

[58] G. Gan, C. Ma, J. Wu, Data clustering: theory, algorithms, and applications, Vol. 20, Siam, 2007.

[59] D. J. Ketchen Jr, C. L. Shook, The application of cluster analysis in strategic management research: an analysis and critique, Strategic management journal (1996) 441–458.

[60] A. M. Turk, Human intelligence through an api (2018). URL `https://www.mturk.com/`

[61] G. A. F. Seber, C. J. Wild, Nonlinear Regression, John Wiley & Sons Incorporated, 2013.

[62] M. Schwaab, E. C. Biscaia Jr, J. L. Monteiro, J. C. Pinto, Nonlinear parameter estimation through particle swarm optimization, Chemical Engineering Science 63 (6) (2008) 1542–1552.

[63] M. Kapanoglu, I. Ozan Koc, S. Erdogmus, Genetic algorithms in parameter estimation for nonlinear regression models: an experimental approach, Journal of Statistical Computation and Simulation 77 (10) (2007) 851–867.

[64] S. Khan, E. Gunpinar, K. M. Dogan, A novel design framework for generation and parametric modification of yacht hull surfaces, Ocean Engineering 136 (2017) 243–259.

[65] T. Fushiki, Estimation of prediction error by using k-fold cross-validation, Statistics and Computing 21 (2) (2011) 137–146.

[66] D. F. Specht, A general regression neural network, IEEE transactions on neural networks 2 (6) (1991) 568–576.

[67] M. R. Sheldon, M. J. Fillyaw, W. D. Thompson, The use and interpretation of the friedman test in the analysis of ordinal-scale data in repeated measures designs, Physiotherapy Research International 1 (4) (1996) 221–228.